



Calhoun: The NPS Institutional Archive
DSpace Repository

Faculty and Researchers

Faculty and Researchers' Publications

1989-12

Plasma wave observations during electron beam experiments at high altitudes

Olsen, R.C.; Lowery, D.R.; Roeder, J.L.

Journal of Geophysical Research; p. 17267-17; (ISSN 0148-0227); 94
<http://hdl.handle.net/10945/60079>

This publication is a work of the U.S. Government as defined in Title 17, United States Code, Section 101. Copyright protection is not available for this work in the United States.

Downloaded from NPS Archive: Calhoun



Calhoun is the Naval Postgraduate School's public access digital repository for research materials and institutional publications created by the NPS community. Calhoun is named for Professor of Mathematics Guy K. Calhoun, NPS's first appointed -- and published -- scholarly author.

Dudley Knox Library / Naval Postgraduate School
411 Dyer Road / 1 University Circle
Monterey, California USA 93943

<http://www.nps.edu/library>

Plasma Wave Observations During Electron Beam Experiments
at High Altitudes

R. C. Olsen and D. R. Lowery

Physics Department, Naval Postgraduate School, Monterey, California 93943

J. L. Roeder

Space Science Laboratory, Aerospace Corporation, Los Angeles, California 90009

Electron beam experiments on the nearly geosynchronous P78-2 satellite conducted in 1979 resulted in observations of intense radiation near the local electron gyrofrequency. These signals resembled naturally occurring fCe waves during the same period. The amplitude of the stimulated waves depended upon beam parameters. During 50 eV beam operations, current levels of 10 pA produced strong emissions. Current levels of 1 pA and 100 pA did not. These emissions correspond in time to previously reported observations of electron distributions which suggest heating of the local thermal plasma. Sufficient power is in the observed emissions to explain the heated electron distributions observed during the experiments.

1. INTRODUCTION

Satellite Charging. Satellite charging is the buildup of static electrical charge on the surface of satellites and has become an important issue in the use of satellite systems. Large negative potentials occur due to an imbalance between ambient electron and ion currents and currents generated by photoemission and secondary electrons. Spacecraft charging effects have been observed on several satellites over the past few years [DeForest, 1972; Garrett, 1981; Grard, 1983; Olsen, 1985]. The large negative potentials that have been induced on geosynchronous satellites have been linked to the satellite failures and unexpected mode changes that have been observed periodically over the past several years. These anomalies can be directly attributed to spacecraft charging effects, which create arcing on the satellite surface, resulting in material breakdown and subsequent failure of the satellite. Motivated by the desire to control charging, experiments were conducted on Applied Technology Satellites 5 & 6 with electron and plasma sources [Olsen,

1981; Olsen, 1985], and on the P78-2 satellite using electron and ion sources [Olsen, 1987]. The latter mission was part of the joint AF/NASA program on Spacecraft Charging at High Altitudes (SCATHA). Charging results from the electron beam experiments have been partially reported by Olsen [1985] and Gussenhoven et al [1981]. Analysis of the particle spectra observed during some electron gun experiments suggested the possibility of electron heating in the near-satellite environment [Olsen, 1987]. This motivated a desire to consider the plasma wave data taken during the electron beam experiments.

Plasma waves and active experiment. An extensive data set on active experiments is emerging after "15 years of research with electron beams in the ionosphere and magnetosphere. The first major series of electron beam emitting vehicles with wave data are the ECHO rockets, as instrumented and launched by the University of Minnesota. Winckler [1980] reviewed the ECHO series and other pertinent experiments, noting the general nature of observed radiation patterns. ECHO 1 results were presented by Cartwright and

Kellogg [1974]. Particularly noteworthy were emissions at the local plasma frequency (or upper hybrid resonance frequency) and twice the gyrofrequency (e.g., Bernstein mode). Signals generated at the second gyroharmonic by the ECHO IV electron beam (840-kV, roughly 100 mA), were strong enough to be detected by ground receivers [Monson and Kellogg, 1978].

An extensive set of rocket experiments have been conducted by Japanese experimenters. Kawashima et al [1982] notes the 7 flights to that point, with beam parameters and noteworthy results. Matsumoto et al [1975] reported on wave phenomena in the VLF range observed by the Japanese sounding rocket K-9M-41. A low energy electron beam was used to investigate the non-linear wave and particle interactions in the ionospheric plasma. Triggered emissions at frequencies around the lower hybrid resonance frequency were found. Kawashima, et al [1987] reported VLF waves excited by electron beam operations on the Japan-US tethered rocket experiment CHARGE-2.

The French-Russian ARAKS experiments were sounding rocket payloads with 0.5 and 1.0 A beams at 15 and 27 keV [Gendrin, 1974]. The experiments were conducted over the Kerguelen Islands, at 100-200 km on 26 January 1975 and 15 February 1975. Cesium plasma sources (hollow cathodes) were included, for current neutralization [Cambou et al, 1980]. The ARAKS experiments results in measurements of emissions at the plasma frequency and twice the gyrofrequency, during both flights. Similar spectra had been noted during the ECHO flights [Lavergnat et al, 1980]. In the VLF frequency range, the principal results was the observation of waves which were most likely a resonance at the local lower hybrid resonance frequency, as modified by the presence of the cesium plasma created by the hollow cathodes [Dechambre et al, 1980].

Stimulated plasma waves in the VLF range are reported by Akai (ISAS

RN285) and Kawashima et al [1981, 1982] for experiments on the Japanese satellite, Jikiken (EXOS-B). EXOS-B was in a relatively low orbit (compared to SCATHA), but at similar L, and hence in similar plasma environments. Electron gun experiments were conducted to study wave excitation phenomena (both linear and non-linear) due to beam-plasma interactions, and to control satellite potential by electron beam emission. The electron gun current was stepped from .25 - 1.0 mA in .25 mA increments. The gun voltage was stepped from 100 to 200 volts in 25 volt increments. The plasma waves were classified by type based on the L-region in which they were observed. Waves at the electron gyrofrequency and its harmonics, the upper hybrid resonance frequency and the plasma frequency were observed.

Experiments on ISEE-1 used beam currents of 10-60 pA and beam energies of 0-40 eV. This is comparable to SCATHA data we will present. Lebreton et al [1982] reported the enhancement of the electric wave spectrum by the injection of an electron beam on ISEE-1. No clearly identified resonances were reported. Koons and Cohen [1982] reported some of the electrical discharges stimulated by the electron beam on SCATHA. Correlation between a change in gun parameters and a change to the spectrum was noted. Electrostatic emissions above the electron gyrofrequency were detected on the electric antenna. The work presented in this paper extends these results.

Plasma waves at the plasma frequency and at the electron gyrofrequency generated in the laboratory are discussed by Bernstein et al [1975]. Electron beam-plasma interactions are of interest, but tend to deal with the beam plasma discharge which involves a neutral gas background.

There are numerous reports in the literature of naturally occurring emissions at or near the electron gyrofrequency [e.g. Koons and Edgar,

1985]. Although the dispersion relation for electron gyrofrequency harmonic waves does not have a solution at exactly the gyrofrequency, Koons and Edgar [1985] report detection of emissions by the VLF receiver on SCATHA at and just above the local electron gyrofrequency. They concluded that present theories could not account for the waves that were the subject of their report. This article will present the plasma wave data taken over a day long period when active experiments with the SCATHA electron gun were being conducted. Identification of plasma waves stimulated by the electron beam at or near the electron gyrofrequency are the major focus of this investigation.

2. THE SCATHA PROGRAM

2.1. SCATHA SATELLITE

The Air Force P78-2 satellite (Figure 1), known as SCATHA for Spacecraft Charging at High Altitude was launched in January 1979 to study causes and dynamics of spacecraft charging processes at geosynchronous orbit. The satellite was launched into a nearly geosynchronous orbit with a period of 23.5 hours at an apogee of 7.3 Re and a perigee of 5.8 Re. The satellite is cylindrical in shape measuring approximately 1.75 meters long and 1.75 meters wide. It is spin stabilized at about 1 rpm with the spin axis in the plane of the orbit and perpendicular to a line between the earth and sun. The instruments are mostly contained in the bellyband and solar cells cover most of the remaining part of the cylinder (Figure 1). The relative locations of the electron gun (SC4-1), magnetic loop (SC1-4) and long electric antenna (SC10-1,-2) are particularly pertinent. The electron gun experiment is described below. Also included in the scientific package were various instruments to measure the potentials existing near the spacecraft and to detect wave and particle emissions. The scientific

instruments are described in detail by Fennell [1982].

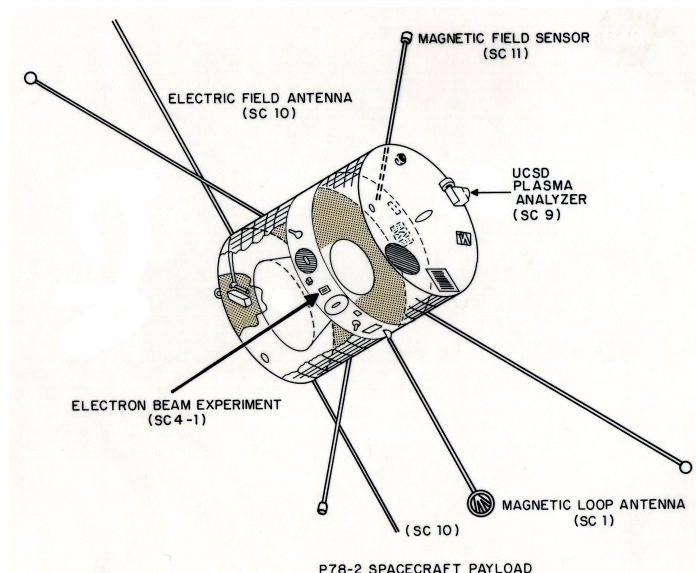


Figure 1. SCATHA space vehicle (P78-2). The electron gun (SC4-1) is on the belly band, on the hidden side of the vehicle.

2.2. ELECTRON GUN

The electron beam system (SC4-1) on SCATHA was designed to emit a stream of electrons over a range of beam currents and energies. The electron beam emitter is basically a power triode tube consisting of an indirectly heated cathode, control grid, focusing assembly and an exit anode at satellite ground. The beam could be operated at currents ranging from 1 pA to 13 mA, and voltage settings from 50 V to 3.0 kV. Duty cycles of 6.25% and 100% were available. The higher current settings were not used due to power restrictions and operational constraints. Currents above 1 mA were not routinely used due to the detrimental effect the beam had on other instrumentation [Gussenhoven et al 1987]. Specifically, severe arcing was noted on the satellite surfaces and resulted in the failure of two of the experiments on 29 March 1979 [Koons and Cohen, 1982]. The

experiments reported below utilized the 10 pA and 100 pA settings, at 50 V.

2.3. DETECTORS

The SC-1 experiment measured VLF and HF emissions and provided the broadband data presented in the spectrograms. The SC-1 experiment employed two antennas, one for electric field measurements and one for magnetic field measurements. The electric antenna was the 100 meter tip to tip dipole used by the electric field (SC10) experiment. The two halves were extended perpendicular to the spin axis. The inner 30 meters of each 50 meter segment was coated with Kapton insulation. The magnetic antenna was an electrostatically shielded air core loop with an effective 575 m² cross section at 1.6 kHz mounted on a

two meter boom off the belly band of the satellite. These antennas were connected to both wide-band and narrow band receivers. The wideband channel could be operated with nominal frequency ranges of 0-3 kHz and 0-5 kHz (depending on telemetry mode). The narrow band receiver had 8 channels, with center frequencies of 0.4, 1.3, 2.3, 3.0, 10.5, 30.0, 100.0, and 300 kHz respectively. These narrowband channels each have relative bandwidths of f7.5%. The instrument was operated with the receivers connected to the electric and magnetic antenna for alternating 16-s intervals. The sensitivity of the magnetic receiver was 3x10⁻⁶ gamma/Hz^{1/2} at 1.3 kHz. The electric field receiver sensitivity was 5x10⁻⁷ V/(m-Hz)^{1/2} at 1.3 kHz and 10⁻⁷ V/(m-Hz)^{1/2} at 10.5 kHz. Each receiver had a 60 dB dynamic range.

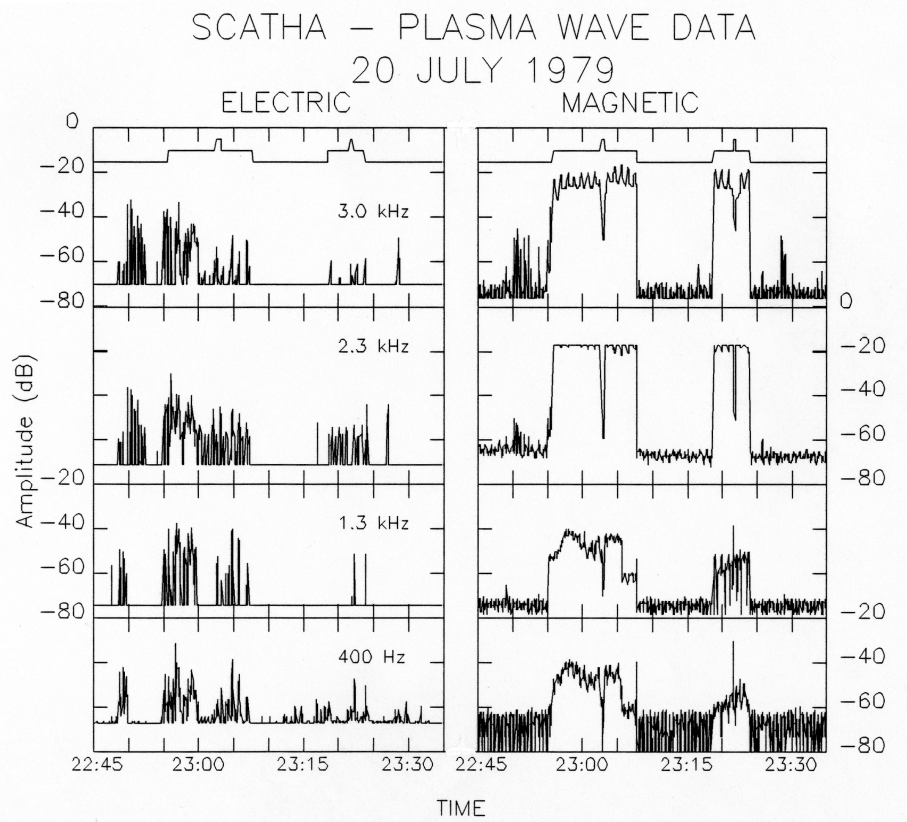


Figure 2. Narrowband electric and magnetic receiver data for 20 July 1979.

Magnetic field data are from the GSFC magnetometer (SC11). The triaxial fluxgate magnetometer was

mounted on a 4 meter boom. Four vector measurements per second were provided, with 0.3 gamma resolution.

The magnetic field data were perturbed by local satellite currents, which introduced an error of up to 1 gamma in the absolute magnetic field measurement [Koons and Edgar, 1985; B. G. Ledley, private communication, 1987].

3. Observations

The observations presented here are the result of a survey of all the available plasma wave data taken during the 1979 electron gun experiments [Lowery, 1987]. The main feature of the data which immediately became apparent was that most electron gun operations resulted in monochromatic emissions at a wide range of frequencies. These emissions were typically constant in frequency with time, varying when the gun current or voltage was changed. The origin of these spectral lines has not been identified, though a reasonable candidate might be a voltage controlled oscillator (VCO) somewhere in the gun. Hence, the majority of the observations do not appear to correspond to interactions between the electron beam and local plasma.

The one major exception to this typical behavior occurred on 20 July 1979 (day 201). A number of low power (50 V, 10–100 pA) experiments were conducted in daylight, at various local times. Monochromatic signals were found which could be attributed to local plasma interactions. This was a magnetically disturbed day with $K_p=4$ for the 2100–2400 period. The satellite was in the dusk bulge at 7.5 RE, $L=8.1$ and magnetic latitude of 6 degrees. As a result of the high magnetic activity, the ambient plasma density was relatively low during these experiments ($n \approx 1 \text{ cm}^{-3}$).

Experiments conducted with the electron gun on 20 July 1979 (day 201), as presented here, were part of a sequence of experiments which resulted in 'real-time' observations of enhanced electron flux above the beam energy. Hence, the cycling of the gun modes was oriented towards understanding the UCSD particle

detector response. Subsequent analysis of the charged particle and electric field data indicate that the spacecraft charged to $N +50$ V during these operations. The electron distribution functions showed evidence that the local plasma (primarily spacecraft generated photoelectrons), and the beam plasma were interacting. The evidence for such interactions was a plateau or flat distribution from 50–70 eV (at the spacecraft). Considerations of phase space invariance showed that this distribution could not be ambient plasma, and must have been locally generated. The data were consistent with heating of the local photoelectron cloud by the beam. One motivation for the work described here was to identify a process which could produce the effect observed in the electron data [Olsen, 1987].

Figure 2 summarizes the 400 Hz – 3.0 kHz electric and magnetic filter data from the SC-1 experiment. The gun current is indicated within the top panels (3.0 kHz). The lowest value is 0 μA (off), intermediate values are 10 μA . The two small peaks at 2302 and 2322 are the 100 pA excursions. The gun on periods are most clearly noticeable in the magnetic channels (right hand side). The most obvious conclusion which appears is that the electron gun causes a 20–30 dB jump in the magnetic receiver output; with a smaller (10 dB) increase in the electric channels. No response was seen in the 4 higher frequency electric channels (10 – 300 kHz).

Further consideration of the figure reveals a number of intriguing points. Gun operations at 10 μA cause the 2.3 kHz channel to saturate, with less extreme increases at the other frequencies. There is a spin modulation which is most obvious in the 3.0 kHz magnetic channel. This point will be addressed later. Increasing the gun current to 100 pA causes a substantial decrease in the stimulated wave response.

The wideband data, recorded from 2241–2330 UT, provide the complimentary frequency spectra

needed to further interpret this plot. Figure 3a shows typical plasma wave data in spectrogram form for this time period. A spectrogram is a grey scale presentation of the plasma wave data, as a function of time and frequency. The vertical axis is frequency from 0 to 3 kHz. The horizontal axis is time. Amplitude of the signal in DB is proportional to the intensity. High amplitude is plotted as black, low amplitude as white, and intermediate values appear as various shades of grey. For example, intense signals can be seen at 0.7 and 2.1 kHz in the magnetic antenna data, denoted by B, in Figure 3a. A less intense signal is found at 1.4 kHz. These interference lines are caused by a 700 Hz tuning fork oscillator that is part of another satellite experiment. These interference lines have been identified previously and have been seen in most data. The receiver is cycled between the electric (denoted by the E in Figure 3) and magnetic antennae (denoted by B) every 16 seconds. Naturally occurring electrostatic electron cyclotron (fCe) waves (the short vertical striations between 2250 and 2252) are observed from about 2.5–2.7 kHz. They are identified by the fact that they occur at or just above the unique frequency, fCe, as calculated from the magnetic field data. From 22:48:30 to 22:50:00 low frequency (less than 300 Hz) signals can be seen in the electric field data. These appear to be naturally occurring signals since they have finite bandwidth. They have not been identified, however. (Note crosstalk—electrostatic emissions are often observed in the magnetic receiver data. It is likely that the observed signals are electrostatic [Koons, and Edgar, 1985; Koons, private communication, 1987]). A summary of the SC4-1 commands is listed in Table I.

All the remaining data from this operation are ordered by icei and we use the measured magnetic field strength from the fluxgate magnetometer to compute and plot fCe

over the spectra. The gyrofrequency was computed at 2 second intervals from the magnetic field strength and plotted on the spectrograms (small dots). Evidence of the magnetic activity can be seen early in the 2241–2330 wideband period in the fluctuation of the magnetic field strength. The naturally occurring electron cyclotron waves (fCe) which begin in Figure 3a at 2250 continue on the next spectrogram (Figure 3b). The naturally occurring waves from 2252 to 2254 (faint vertical stripes) are neatly matched to the calculated time varying gyrofrequency overplotted. These signals are similar in appearance to those which were induced by the electron gun operations.

At 22:52:40 the electron gun system is initialized and it is powered up at 22:54:54. At 22:55:00 the electron gun is turned on. A prompt, if muddled, effect can be seen on the plasma wave data (Figure 3b). The tuning fork related interference lines are masked and a strong broadband signal can be seen in the magnetic field spectrum. At 22:55:37 the electron beam is energized at a current level of 10 pA and 50 eV. The gun was operated continuously in this mode until 23:02:28 when the beam current was increased to 100 pA.

A monochromatic signal, similar to the fCe wave, is observed in the 10 μ A mode. The intense, monochromatic signal above 2 kHz varied in frequency from about 2400 to 2600 Hz as seen in the latter period of Figure 3b. This signal is modulated in frequency at the satellite spin period of 59 sec, has a very narrow bandwidth, and appears monochromatic in the electric data to within receiver resolution. For example, line plots showed a monochromatic signal near 2400 Hz at 22:56:00. The gyrofrequency calculated from the magnetic field strength for this time was 2385 Hz. In the early part of the period after the electron gun was first turned on (22:55:00 – 22:57:00) the signal was at or near the electron gyrofrequency, mimicking the naturally occurring waves. This is

apparently the signal which drives the 2.3 kHz magnetic channel to saturation (Figure 2). Figure 3c shows that significant differences between fee and the signal frequency begin to occur by 22:58:00. In particular, the signal frequency drops substantially below the gyrofrequency (at 22:59:00). This is significant because if the signal is below the local electron cyclotron frequency, it cannot be an electron cyclotron wave. The signal continues for as long as the electron gun is operated in the 10 pA mode. The fluctuation in the frequency of the signal is approximately sinusoidal and is repeatable over several periods. This period is close to or equal to the satellite spin period. Details of the fluctuation in frequency include a 'knee' in the electric field spectrogram (at 23:00:30, arrow on top right in Figure 3c). This is a distinguishable characteristic of the signal and appears in the same general position on the waveform throughout this period.

Significant changes in the plasma wave data result from changes to the gun parameters. From 23:02:28 to 23:03:15 the gun beam current was increased to 100 pA (Figure 3d). The VLF data with the gun on at 100 pA appear similar to the data with the electron beam off. The strong interference lines at 700 and 2100 Hz reappear in the magnetic channel. Close examination of the data indicated that some of the sporadic naturally occurring electron cyclotron waves were present. The intense monochromatic signal seen at 10 pA beam current disappeared. This decrease in the AGC controlled wideband response is confirmed by the filter data shown in Figure 2. This dependence on beam current would indicate a dependence on the density of the beam plasma, since velocity (energy) is constant.

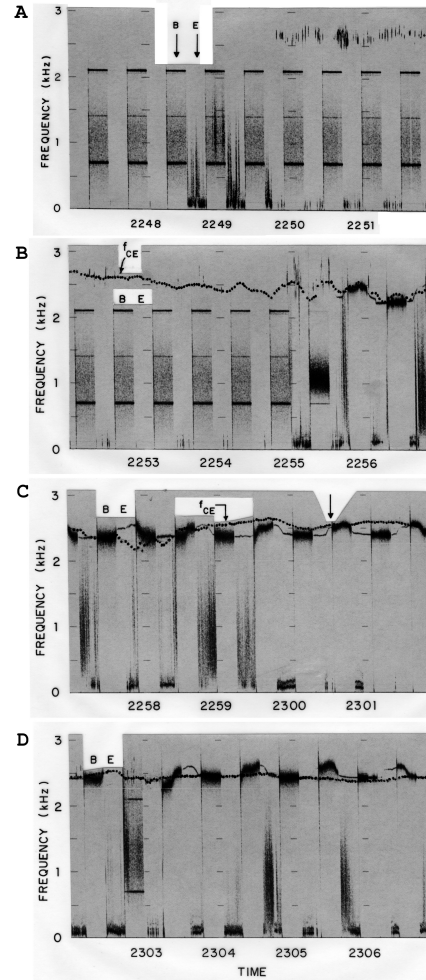


Figure 3. Frequency time spectrograms for the plasma wave data
 a. Illustration of gun off data, showing interference lines at 700, 1400 and 2100 Hz, and naturally occurring fCe waves.
 b. Illustration of natural fCe waves, with fCe overplotted as small dots. Gun on transition (22:55) produces intense signals at fce.
 c. As above, but with signal descending below fce.
 d. From 23:02:28–23:03:15, the gun current is increased to 100 pA. The induced signal at fce disappears.

TABLE 1. Summary of the SC4-1 Commands

Universal Time	SC4-1 Command
2253:40	initialize and off
2254:54	system on
2255:00	beam on
2255:37	beam current to 10 μ A
2302:28	beam current to 100 μ A
2303:15	beam current to 10 μ A
2307:41	beam off
2318:31	beam on 10 μ A
2321:34	beam current to 100 μ A
2321:58	beam current to 10 μ A
2323:48	beam off
2326:03	system initialization and off

Data are from July 20, 1979 (day 201).

At 23:03:15 the beam current was reduced to 10 pA and the VLF characteristics returned to those previously observed at 10 pA beam current (i.e. the 2.4–2.7 kHz signal was again present). The system remained in this configuration until 23:07:41 when the electron beam was turned off. The VLF characteristics reverted to those observed prior to the gun operations (prior to 22:55:00). The 700, 1400 and 2100 Hz interference lines returned. For the next 10–12 minutes the electric spectra revealed no obvious signals, and the magnetic antenna showed only the tuning fork lines and receiver noise. The repeatability of the effects of the electron gun operations were emphasized by repetition of the sequence. At 23:18:31 the electron beam was again turned on at 10 pA beam current. The VLF data resumed the behavior shown previously. The signal oscillating between 2400–2600 Hz returned and the low frequency signal (100–200 Hz) became more intense. From 23:21:34 to 23:21:58 the beam current was increased to 100 μ A, and again the 2400–2600 Hz signal disappeared and the interference lines reappeared in the magnetic data. At 23:21:58 the beam current was reduced to 10 pA and the VLF data regained their familiar character. At 23:23:48 the electron beam was turned off and the 700, 1400 and 2100 Hz interference lines could again be seen in the magnetic receiver data. Also sporadic electron gyrofrequency emissions were present.

4. DISCUSSION

The 2.4–2.7 kHz signal that is observed during the 10 pA mode of operation is strongly linked in frequency characteristics to electron cyclotron waves, near but not at the natural cyclotron frequency. This signal is the dominant effect that was seen in the VLF data during this gun operation and we attempt here to explain the source of this apparently stimulated electron cyclotron wave. The apparent broadness of the signal in the magnetic field data is a result of the AGC control on the satellite and the processing system. Although this signal appears to have a finite bandwidth, it is most likely the same monochromatic signal observed by the electric antenna. The relatively constant amplitude suggests that the satellite itself is the source of the signal. Since the signal is only visible at 10 pA beam current, there are apparently beam-plasma effects which determine the propagation of the signal to the electric and magnetic antennas through the ambient plasma. Theory holds that there should be no signals below the gyrofrequency due to the dispersion relations. The fact that the oscillation drops below the calculated gyrofrequency is disturbing. Since the signal is close to f_{ce} we pursued the idea that there was something causing the magnetic field strength near the satellite to vary. One thing that might perturb the satellite magnetic field is the solar array current.

Figure 4 shows the solar array current, I_{sa} , plotted with the frequency of plasma wave oscillation seen on 20 July 1979. Also plotted is the amplitude of the signal in the 3 kHz magnetic channel. The solar array current is obviously modulated at the satellite spin period. This is a result of shadowing of the solar cells as the booms pass between the satellite and the Vii. The similarity of the shape of the solar array current to the variation in the SC-1 signal frequency and amplitude is strong. We suggest that the solar array current causes a perturbation to the total magnetic field. This

field is largely balanced out by design, but is non-zero. The perturbation field, or satellite magnetic moment, will vary with the solar array current, I_{sa} . The perturbation in the magnetic field strength near the satellite then results in a slight change in the electron gyrofrequency. (AB or $A I_{sa}$, Ofce a AB).

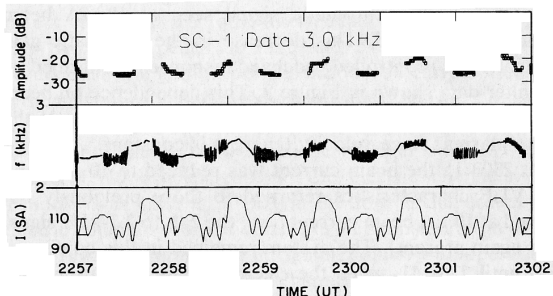


Figure 4. (Top) Signal from 3.0 kHz channel, magnetic antenna. (Middle) Frequency of intense signal in wideband data. (Bottom) Solar array current, as modulated by the satellite spin.

The question of where to evaluate the magnetic field is raised at this point. The two possibilities are the source, or generation region for the waves, and the antenna, or reception region. Note in figure 3, that there is no shift in the frequency of the received signal when the antenna are switched. This implies that either both the electric and magnetic loop antenna are coupling at the same location, which seems unlikely, or they are responding to a source at a constant frequency. This source region would be the beam-plasma interaction region, which is probably quite close to the satellite (e.g., within 1 meter).

The measured magnetic field is obtained from sensors at the end of a 4 meter boom. The value of the magnetic field at the magnetometer is known to have an error of a few gamma due to satellite generated fields (B. Ledley, private communication, 1987). Hence, a perturbation field of 10 gamma near the satellite surface,

dropping to a few gamma at 4 meters, is consistent with a fluctuation in ice of 280 Hz. A net, unbalanced, current fluctuation of 0.1 – 1.0 A should be able to produce a field of 10 gamma (nano-Tesla), dropping as $1/r^3$ away from the solar array. This could account for the cyclotron emission appearing below the gyrofrequency. The oscillation varies in frequency by only a few hundred hertz. The magnetic intensity would only have to produce this change, well within our estimates. Note again that the modulation of the solar array current closely matches the shape of the modulation of the plasma wave data (Figure 4). The modulation of the 3kHz data can be understood as movement of the signal frequency in and out of the passband for that channel.

We observed similar behavior in the plasma wave data over several operational periods on this day. No other clear examples of f_{ce} related emissions have yet been found on other days. This is primarily due to the abundance of satellite/gun generated interference lines which typically appeared in the data, as described in the introduction to the observations.

These interference lines occurred in two categories. The first category was comprised of multiple signals, typically varying wildly in frequency over time periods of seconds. The second category consisted of signals which were constant in frequency, for a given gun mode, changing as gun current or voltage changed. The element of the day 210 data, shown here, which ultimately makes these signals identifiable is the spin modulation, which is not normally evident in the SC-1 data.

It was partly accidental that this characteristic of the data was identified, and made obvious by reprocessing on the compressed time scale used for the plots in Figure 3.

Note that the satellite body was charged to +50 V by the gun operation. This has the effect of limiting the beam, but also of

causing the incoming electron flux (ambient electrons) of acquiring a beam-like distribution function, in the spacecraft frame of reference. Hence, the plasma distributions around the satellite are presumably unstable due both to the emitted beam, and the incoming 'beam'.

V. CONCLUSIONS

On Day 200 the electron gun stimulated an emission at the local electron gyrofrequency when operated at 10 pA, 50 volts. This signal resembled naturally occurring fCe waves during the same period. Fluctuations in the frequency of the signal correlated with satellite spin and solar array current variations, indicating that the signal is a result of interactions between the electron beam and local plasma. The waves were clearly affected by the selected current level, indicating a dependence on N_{beam} vs. N_{ambient} . These plasma wave observations correspond to measurements of the plasma data reported by Olsen [1987]. In the electron data, evidence for heating of the ambient plasma was found. It is evident that substantial wave power is available to couple the beam energy into the local plasma, if a suitable mechanism can be worked out. As a result of this work, operations were scheduled for the final orbits of ISEE-1 in summer, 1987. The electron gun was operated from the magnetopause in to perigee. Studies of these data are just beginning, but should resolve the fCe dependence found here, with the advantage of higher frequency range (e.g, up to the plasma frequency).

ACKNOWLEDGEMENTS

This work was conducted with funds administered by the Naval Postgraduate School Research Council and NASA Lewis Research Center. The work at the Aerospace Corporation was supported by the U.S. Air Force Systems Command's Space Division under Contract F04701-85-C-0086. The plasma wave data were obtained from the PI, Dr. Harry Koons of Aerospace

Corporation. The PI for the electron gun, Mr. Herb Cohen labored mightily to operate the experiment, and has provided substantial help in recognizing and interpreting electron gun operating modes. Ms. Delia Donatelli did a substantial amount of work on the plasma wave data (unpublished) from which we have benefited. These data are from a series of experiments conducted with the unending support and patience of the AF/SCF personnel.

REFERENCES

- Akai, K., Electron Beam-Plasma Interaction Experiment in Space, ISAS Research Note 285, The Institute of Space and Astronautical Science, Komaba, Meguro-ku, Tokyo, Japan, ca, 1984.
- Bernstein, W., et al., Laboratory observations of RF emissions at ω_{pe} and $(n + 1/2)\omega_{ce}$ in electron beam-plasma and beam-beam interactions, *J. Geophys. Res.*, 80, 4375-4379, 1975.
- Cambou, F., V. S. Dokoukine, J. Kavergnat, R. Pellat, H. Reme, A. Saint-Marc, R. Z. Sagdeev, and I. A. Zhulin, General description of the ARAKS experiments, *Ann. Geophys.*, 36, 351-356, 1980.
- Cartwright, D. G., and P. J. Kellogg, Observations of radiation from an electron beam artificially injected into the ionosphere, *J. Geophys. Res.*, 79, 1439-1457, 1974.
- Dechambre, M., J. Lavergnat, and R. Pellat, Waves observed by the ARAKS experiments: The VLF range, *Ann. Geophys.*, 36, 351-356, 1980.
- DeForest, S. E., Spacecraft charging at synchronous orbit, *J. Geophys. Res.*, 77, 651-659, 1972.
- Fennell, J. F., Description of the P78-2 (SCATHA) satellite and experiments, in *The IMS Source Book: Guide to the International Magnetospheric Study Data Analysis*, edited by C. T. Russell and D. J. Southwood, p. 65, AGU, Washington, D. C., 1982.
- Garrett, H. B., The charging of spacecraft surfaces, *Rev. Geophys.*, 19, 577-616, 1981.
- Gendrin, R., The French-Soviet "ARAKS" experiment, *Space Sci. Rev.*, 15, 905-931, 1974.
- Grard, R., K. Knott, and A. Pedersen, Spacecraft charging effects, *Space Sci. Rev.*, 34, 289-304, 1983.
- Gussenhoven, M. S., H. A. Cohen, D. A. Hardy, W. J. Burke, and A. Chesley, Analysis of ambient and beam particle characteristics during the ejection of an electron beam from a satellite in near-geosynchronous orbit on March 30, 1979, *Spacecraft Charging Technology*, 1980, *NASA Conf. Pub.* 2182, 642-664, 1981.
- Gussenhoven, M. S., E. G. Mullen, and D. A. Hardy, Artificial charging of spacecraft due to electron beam emission, *IEEE Trans. Nucl. Sci.*, NS-34, 1614-1619, 1987.
- Kawashima, N., A. Ushikoshi, Y. Murasato, A. Morioka, H. Oya, M. Ejiri, S. Miyatake, and H. Matsumoto, Beam-plasma interaction experiment in the magnetosphere by emitting an electron beam from satellite Jikiken (EXOS-B), *J. Geomagn. Geoelectr.*, 33, 145-159, 1981.
- Kawashima, N., and Jikiken (EXOS-B) CBE Project Team, Wave excitation in electron beam experiment on Japanese satellite "Jikiken (EXOS-B)," in *Artificial Particle Beams in Space Plasma Studies*, edited by B. Grandel, pp. 101-110, Plenum, New York, 1982.
- Kawashima, N., S. Sasaki, K. I. Oyama, W. J. Raitt, P. R. Williamson, and P. M. Banks, Further analysis of the results from a series of tethered rocket experiments, in *Space Tethers for Science in the Space Station Era*, edited by L. Guerriero and I. Bekey, pp. 76-81, Societa Italiana di Fisica, Bologna, Italy, 1988.
- Koons, H. C., and H. A. Cohen, Plasma waves and electrical discharge stimulated by beam operations on a high altitude satellite, in *Artificial Particle Beams in Space Plasma Studies*, edited by B. Grandel, pp. 111-120, Plenum, New York, 1982.
- Coons, H. C., and B. C. Edgar, Observations of VLF emissions at the electron gyrofrequency, *J. Geophys. Res.*, 90, 10,961-10,967, 1985.
- Koons, H. C., B. C. Edgar, J. F. Fennell, and D. J. Gorney, Observations of electron cyclotron harmonics emissions associated with field-aligned electron beams, *J. Geophys. Res.*, 92, 7531-7537, 1987.
- Lavergnat, J., M. Dechambre, R. Pellat, Y. V. Kushnerevsky, and S. A. Pulnits, Waves observed by the ARAKS experiments: Generalities, *Ann. Geophys.*, 36, 323-332, 1980.
- Lebreton, J. P., R. Torbert, R. Anderson, and C. Harvey, Stimu-

- lation of plasma waves by electron guns on the ISEE-1 satellite, in *Artificial Particle Beams in Space Plasma Studies*, edited by B. Grandal, pp. 133-146, Plenum, New York, 1982.
- Lowery, D. R., Survey of the Air Force P78-2 (SCATHA) satellite plasma wave data during electron gun operations, M.S. thesis, Nay. Postgrad. Sch., Monterey, Calif., 1987.
- Matsumoto, H., S. Miyatake, and I. Kimura, Rocket experiment on spontaneously and artificially stimulated VLF plasma waves in the ionosphere, *J. Geophys. Res.*, **80**, 2829-2834, 1975.
- Monson, S. J., and P. J. Kellogg, Ground observations of waves at 2.96 MHz generated by an 8- to 40-keV electron beam in the ionosphere, *J. Geophys. Res.*, **83**, 121-131, 1978.
- Olsen, R. C., Modification of spacecraft potentials by thermal electron emission on ATS-5, *J. Spacecr. Rockets*, **18**, 527-532, 1981.
- Olsen, R. C., Experiments in charge control at geosynchronous orbit-ATS-5 and ATS-6, *J. Spacecr. Rockets*, **22**, 254-264, 1985.
- Olsen, R. C., Electron beam experiments at high altitudes, *J. Electrostat.*, **20**, 43-57, 1987.
- Winckler, J. R., The application of artificial electron beams to magnetospheric research, *Rev. Geophys.*, **18**, 659-682, 1980.
- D. R. Lowery and R. C. Olsen, Physics Department, 61-Os, Naval Postgraduate School, Monterey, CA 93943.
- J. L. Roeder, Space Science Laboratory, Aerospace Corporation, Los Angeles, CA 90009.

(Received March 28, 1989; revised June 12, 1989; accepted July 25, 1989.)